www.czasopisma.pan.pl PAN POLSKA AKADEMIA NAUK www.journals.pan.pl

A R C H I V E S O F M E T A L L U R G Y A N D M A T E R I A L S

Volume 57 2012 Issue 4

DOI: 10.2478/v10172-012-0115-3

H. SOLOMON*, N. SOLOMON**

EFFECT OF CRYSTALLIZATION ON THE ELECTRICAL RESISTANCE AND STRUCTURE OF AMORPHOUS Fe-Co-Cr-B-Si ALLOYS

WPŁYW KRYSTALIZACJI NA OPORNOŚĆ ELEKTRYCZNĄ I STRUKTURĘ AMORFICZNYCH STOPÓW Fe-Co-Cr-B-Si

The goal of this paper is to present the influence of temperature variation and iron substitution with Co on the structure and electrical properties of amorphous $Fe_{75-x}Co_xCr_1B_7Si_{17}$ alloys (where x=1, 4, 7, and 10 at.%), obtained by melt-spinning technique.

The electrical resistivity of the samples was measured by using a usual four-probe method from -160°C to 750°C. The electrical resistivity was also measured at room temperature for the amorphous $Fe_{75-x}Co_xCr_1B_7Si_{17}$ ribbons annealed at various temperatures for different holding time.

The annealed samples were also investigated by Vickers microhardness test. The amorphous structure of tested materials was examined by X-ray diffraction (XRD), Mössbauer spectroscopy, differential scanning calorimetry (DSC) and scanning electron microscopy (SEM) methods. Experimental results confirmed the utility of applied investigation methods and the influence of the Co content and annealing process on the crystallization, structure and electrical properties of examined amorphous alloys.

Keywords: amorphous alloys, X-ray diffraction, electric resistivity, microhardness, annealing

Celem niniejszego artykułu jest przedstawienie wpływu zmian temperatury i zastąpienia Fe przez Co na strukturę i właściwości elektryczne amorficznych stopów $Fe_{75-x}Co_xCr_1B_7Si_{17}$ (gdzie x=1, 4, 7, 10 at.%) odlewanych na wirującym dysku. Oporność elektryczna próbek była mierzona metodą czteropunktową w zakresie od -160°C to 750°C. Oporność elektryczną zmierzono także w temperaturze pokojowej dla amorficznych taśm $Fe_{75-x}Co_xCr_1B_7Si_{17}$ wyżarzonych w różnych temperaturach dla różnych czasów.

Wyżarzone próbki poddano również badaniom mikrotwardości Vickersa. Amorficzną strukturę badanych materiałów badano przy użyciu dyfrakcji rentgenowskiej (XRD), spektroskopii Mössbauera, różnicowej kalorymetrii skaningowej (DSC) oraz skaningowej mikroskopii elektronowej (SEM). Wyniki eksperymentu potwierdziły przydatność zastosowanych metod badawczych oraz wpływ zawartości Co i wyżarzania na proces krystalizacji, strukturę i właściwości elektryczne badanych stopów amorficznych.

1. Introduction

Amorphous Fe-Co based metallic alloys are a novel group of advanced engineering materials. In spite of their disordered atomic-scale structure specific to amorphous alloys, Fe-Co based metallic glasses exhibit specific thermal, corrosion, electrical and magnetic properties which allow their practical applications in various fields of technology. Due to their special properties Fe-Co based metallic glasses are suitable materials for many electrical devices such as sensors, band-pass filters, magnetic wires, electric power transformers [1, 2]. There are also several, actual and potential, applications of metallic glasses as structural materials, e.g. knife edges, springs, parts of the sport goods (golf-club heads, tennis racket frames), information storage and reproduction devices, application in fashion industry [3]. However, there are several limiting factors: high cost of components and processing, brittleness, instability above Tx (Tx stands for temperature of crystallization), which limit their applicability.

Crystallization of metallic glasses occurs when they are heated at temperatures high enough to overcome the energy barrier between their metastable amorphous state and crystalline one. In many cases this process takes place in several steps, involving intermediate metastable

* "DUNAREA DE JOS" GALATI UNIVERSITY, 47 DOMNEASCA STREET, 800008 GALATI, ROMANIA

** "STEFAN CEL MARE" SUCEAVA UNIVERSITY, 13 UNIVERSITII STREET, 720229 SUCEAVA, ROMANIA

phases before reaching the final crystalline stable state. These structural changes during crystallization process are reflected in the evolution of several physical properties of metallic glasses [4].

In addition to their special properties such as low volume shrinkage, high mechanical strength and hardness, low surface roughness the amorphous metallic alloys exhibit excellent electrical properties. The electrical resistivity as a function of temperature is a characteristic for a wide variety of metallic glasses and it was subject in a lot of investigations [4, 5, 6; 7]. Depending on temperature the electrical resistivity shows a series of anomalies, especially around temperatures where first or second range transitions take place [8]. It is know that electrical resistivity is sensitive to the microstructure development in solid state [4].

At low temperatures the electrical resistivity should tend to zero, but due to the structure defects and impurities, it tends to a constant value. If the impurities presented in a certain metal have an electronic spin, then the electrical resistivity shows a minimum or a maximum characteristic. This type of resistivity anomaly as a minimum at low temperature, known as Kondo effect, has been found in many amorphous alloys [5].

Rein et al. [9] have studied the thermal variation of electrical resistivity of some alloys of Metglas-system within the temperature range of 1.5 to 800 K, as well as the influence of the crystallization on the electrical resistivity. In the case of Metglas alloys was noticed that the crystallization causes the further modification of the minimum electrical resistivity [10, 11].

Annealing at temperatures lower than the glass transition temperature, the amorphous alloys experience a structure relaxation which must be clearly distinguished from crystallization process. The structure relaxation process is connected with local atomic rearrangements, decreasing of free volume and the glass changes from a less stable to a more stable, but still metastable state [12, 13].

The aim of this paper is to provide a structural, mechanical and electrical properties analysis of the amorphous Fe-Co-Cr-B-Si alloys, using X-ray diffraction (XRD), Mossbauer spectroscopy, differential scanning calorimetry (DSC), and scanning electron microscopy (SEM) methods.

2. Experimental Procedure

The amorphous $Fe_{75-x}Co_xCr_1B_7Si_{17}$ (x=1, 4, 7, and 10 at.%) alloys were prepared by melt spinning technique in pure argon atmosphere, in form of ribbons having a thickness of 25-32 μm and a width of about 2 mm.

The amorphous structure of the samples has been examined by X-ray diffraction. Scanning electron microscopy and Mössbauer spectroscopy, which is a technique that provides us with simultaneous information namely on the structural arrangement and magnetic microstructure, were also used for samples characterization.

In order to prepare stable amorphous alloys under given conditions for perspective applications it is desirable to understand the mechanisms by which a metallic glass crystallizes.

The as quenched ribbons were annealed in the first stage for 30 minutes exposure time at temperature T_a ranging from 200°C to 500°C. The thermal stability associated with crystallization temperature of the amorphous $Fe_{75-x}Co_xCr_1B_7Si_{17}$ (x=1, 4, 7, and 10 at.%) alloys were measured using the differential scanning calorimetry (DSC) at heating rates of 5 and 10°C/min. under an argon atmosphere.

The dependence between electrical resistivity, temperature and cobalt content, was measured using samples of amorphous $Fe_{75-x}Co_xCr_1B_7Si_{17}$ alloys. Electrical resistivity versus temperature was measured between -160 and 750°C using constant heating rates as above mentioned. Therefore, four-probe electrical resistivity measurement was conducted in an argon-atmosphere tube furnace with temperature fluctuation less than 2°C for the range from 0 to 750°C. To determine the resistivity values at low temperatures from -160 to 0°C, the samples were immersed in liquid nitrogen. During the measurement a platinum thermocouple with the measuring range spanning values from -250 to 850°C was used. A Wheatstone bridge was used to determine samples resistivity values which were recorded at 10°C interval.

3. Results and discussion

The amorphous nature of the samples was confirmed metallographic and by X-ray diffraction studies using Cu- Kα radiation. The diffraction pattern of studied ribbon samples is characterized by the typical halo indicating that the as-cast samples are in the amorphous state [11, 14], Fig. 1.

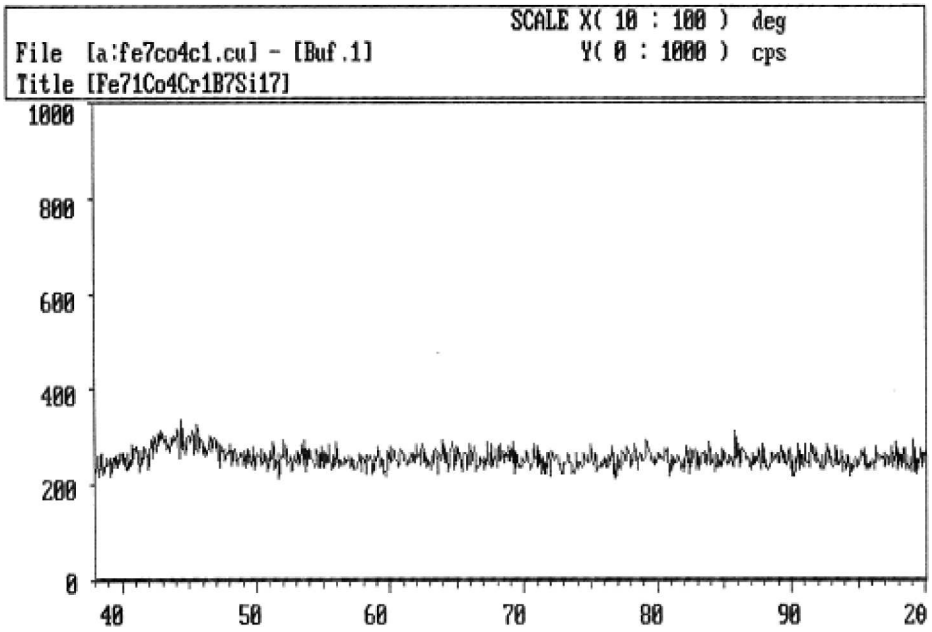

Fig. 1. $Fe_{71}Co_4Cr_1B_7Si_{17}$ alloy X-ray diffraction diagram

The SEM image, Fig. 2, implies no crystal structure and confirms again that the as-cast alloys are in the amorphous state.

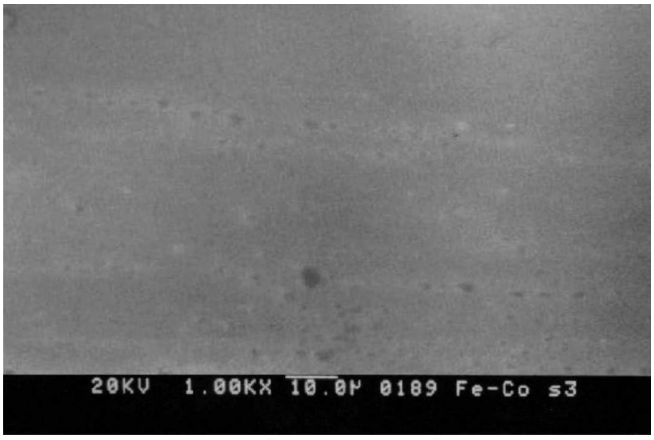

Fig. 2. SEM microstructure of an as-cast $Fe_{75-x}Co_xCr_1B_7Si_{17}$ ribbon

Many amorphous alloys exhibit a high thermal stability. Therefore, samples of each alloy belong to amorphous Fe-Co-Cr-B-Si system were submitted to heat treatments. Subsequent heat treatments at 200, 250, 300, 350, 400, 450, 500°C; with exposure time of 30 minutes, in a neutral furnace atmosphere (Ar) were applied.

The heat treated samples were again subject to diffraction analysis and Mössbauer spectroscopy. The Mössbauer spectrum for the amorphous $Fe_{71}Co_4Cr_1B_7Si_{17}$ alloy at room temperature, after heating at 250°C and 420°C for 30 minutes, is shown in Fig. 3. A well defined sextet shows that the local environment of the Fe is ordered by the annealing process [15-17]. Fig. 3a shows that after heating at 250°C the annealed specimens are still in amorphous state.

The diffraction analysis diagrams of the annealed samples below to 450°C (Fig. 4a), show that they exhibit the same broad symmetric halo, as in quenched state, which is typical for a fully amorphous phase, indicating that the material remained in amorphous state after heat treatment and demonstrating in the same time that Fe-Co-Cr-B-Si system exhibits a high thermal stability [11]. In the case of the sample annealed at 450°C (Fig. 4b) the structure is still predominantly amorphous (see also Fig. 3b), but shows evidence of crystalline precursors [18]. It could be noted that the heat treatment of amorphous alloy $Fe_{71}Co_4Cr_1B_7Si_{17}$ at 500°C for 30 minutes certainly result in some new chemical compounds [16].

The investigation carried out by Quivy et al [19] with respect to crystallization of the amorphous alloys Fe-B-Si-C indicates that this takes place in two stages.

According to [19] after annealing for 30 minutes at 450°C the first crystallization stage is completed. This stage corresponds to the appearance in the amorphous matrix of some Fe dendrites with low Si content, less than 1%. The second stage consists in the crystallization of the residual amorphous matrix enriched in B, Si, C which, subsequently becomes non-homogenous.

In the case of Fe-Co-Cr-B-Si samples, the phases of Fe(Si), Fe_2B and Fe_3B appear simultaneously between the Fe_α dendrites in the form of stratified crystals [14].

The composition of our alloys is not identical; however the transformation temperatures are very similar.

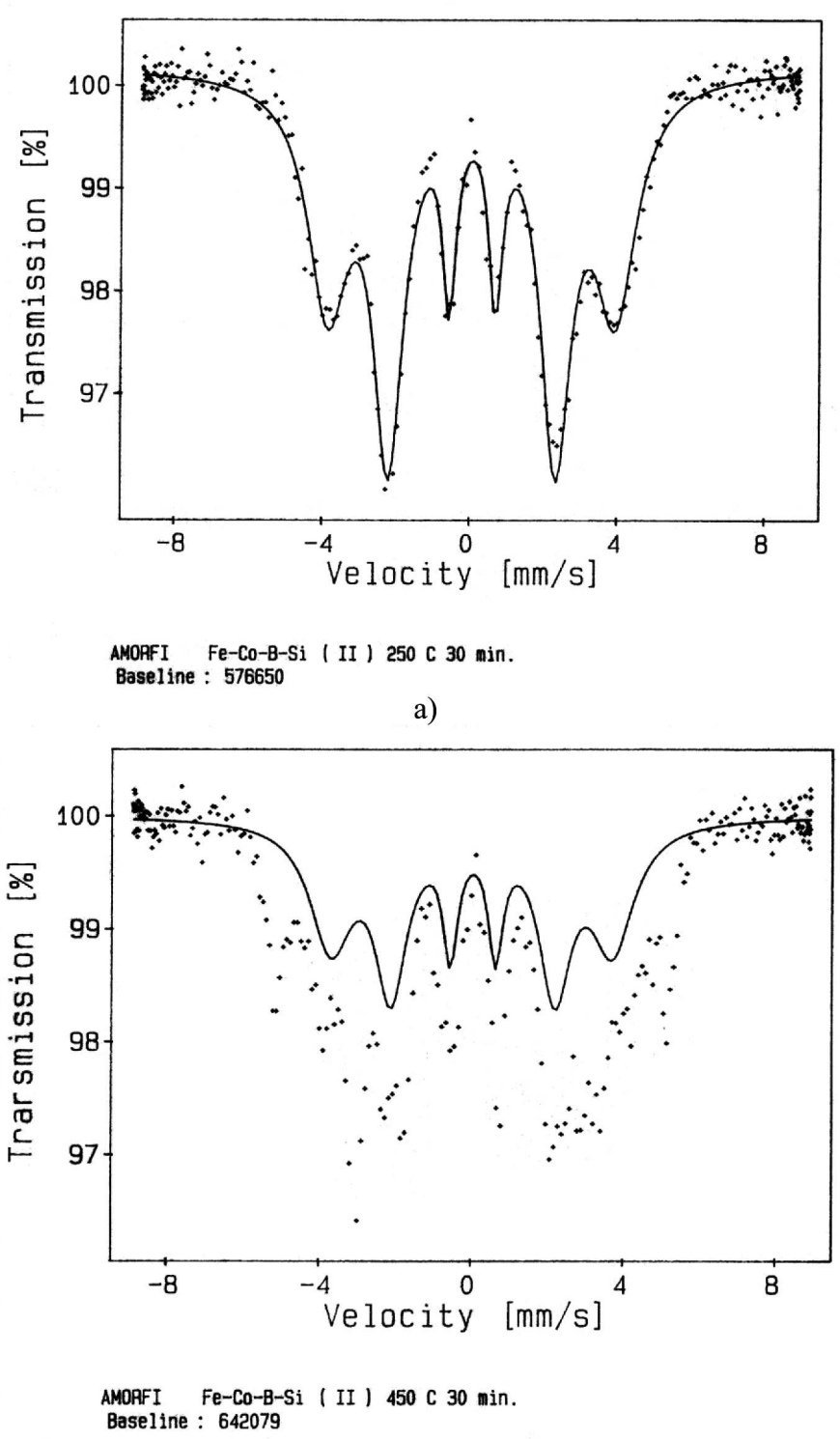

Fig. 3. Mössbauer spectrum measured at 20°C of amorphous $Fe_{71}Co_4Cr_1B_7Si_{17}$ alloy after heating at 250°C (a) and 450°C (b) respectively for 30 minutes, heating rate of 5°C/min

The microstructure and Roentgen analyses reveal crystals of some compounds only after annealing at 500°C for 30 minutes. Applying annealing at lower temperatures, even at longer times of exposure (60 or 90 minutes) does not modify the structure (Fig. 3a and Fig. 4a).

In agreement with the X-ray findings, thin sheet of annealed specimens at 500°C were found to contain FeB crystals in the amorphous matrix (Fig. 4b).

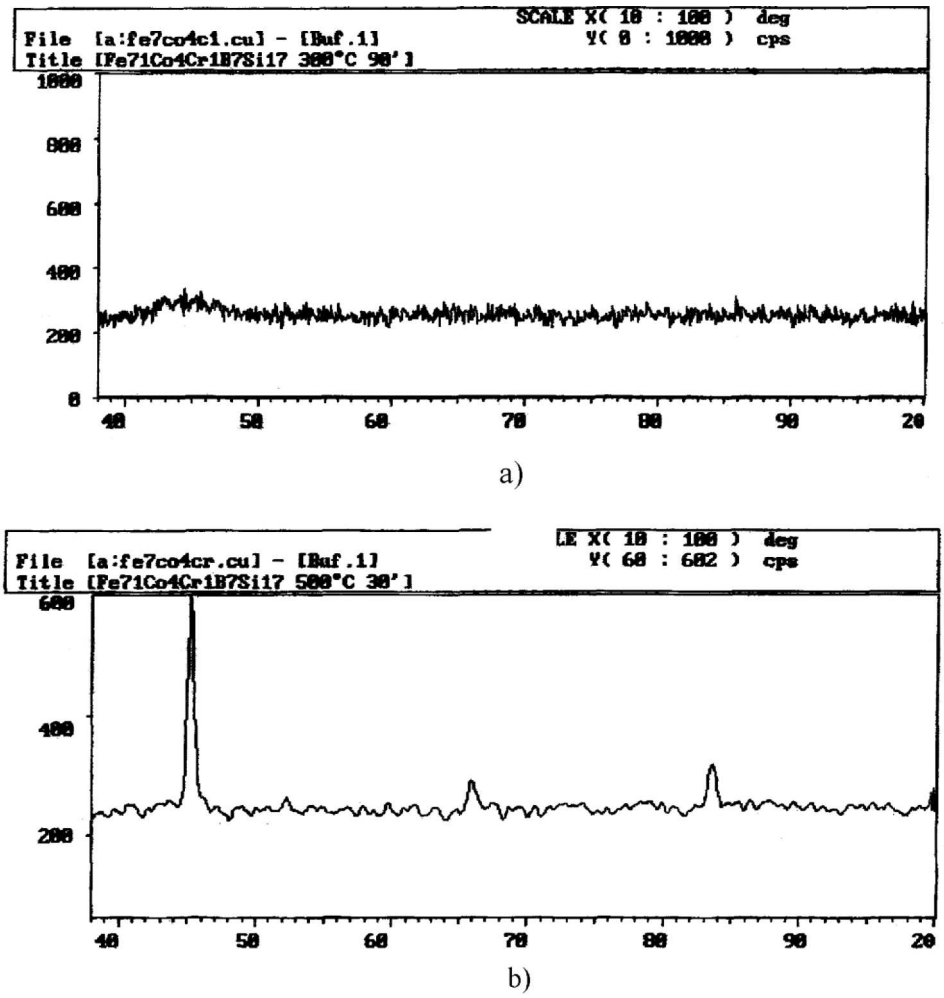

Fig. 4. X-ray diffraction diagrams of heat treated amorphous $Fe_{71}Co_4Cr_1B_7Si_{17}$ alloy a) 90 minutes at 300°C; b) 30 minutes at 500°C

Fig. 5 presents SEM microstructure of the amorphous $Fe_{71}Co_4Cr_1B_7Si_{17}$ alloy annealed at 500°C for 30 minutes. The number and size of FeB crystals increases with annealing time. Despite structural relaxation which occurs rapidly during the first step of annealing, the as quenched $Fe_{74}Co_4Cr_1B_7Si_{17}$ alloy remains thermally stabile up to 430°C where the first crystallization stage appears. This results in primary crystallization of nanocrystalline bcc-Fe phase. A second crystallization stage appeared at the temperature up to 535°C.

For identifying the primary and secondary crystallization temperatures, T_{x1} and T_{x2}, respectively, of the amorphous $Fe_{75-x}Co_xCr_1B_7Si_{17}$ alloys, differential scanning calorimetry was used. Two heating rate of 5°C/min and 10°C/min during the annealing process have been applied.

Based on DSC curves of amorphous $Fe_{75-x}Co_xCr_1B_7Si_{17}$ alloys (x=1, 4, 7, and 10 at.%) the critical temperatures have been obtained. On each

Fig. 5. SEM microstructure of a sample annealed at 500°C for 30 minutes, 500X

DSC curve two exothermic peaks have been detected, the first one being the most intense [20].

Table 1 shows the value of critical temperatures for all amorphous $Fe_{75-x}Co_xCr_1B_7Si_{17}$ alloys (x=1, 4, 7, and 10 at.%):

TABLE 1

Critical temperature

Alloy type	Heating rate, °C/min	Heating temperature, °C	Critical temperature, °C	
			T_{x1}	T_{x2}
$Fe_{74}Co_1Cr_1B_7Si_{17}$	10	800	431	545
	5	1000	419	527
$Fe_{71}Co_4Cr_1B_7Si_{17}$	10	800	439	548
	5	1000	428	535
$Fe_{68}Co_7Cr_1B_7Si_{17}$	10	800	443	552
	5	1000	435	543
$Fe_{65}Co_{10}Cr_1B_7Si_{17}$	10	800	450	554
	5	1000	442	546

TABLE 2

Electrical resistivity variation

Resistivity, [10^{-6} Wm] / Temperature, °C	Amorphous $Fe_{75-x}Co_xCr_1B_7Si_{17}$ (x=1, 4, 7, and 10 at.%) alloys as quenched			
	X=1	X=4	X=7	X=10
-160°C	1.47	1.56	1.87	1.98
20°C	1.52	1.62	1.88	1.98
400°C	1.98	1.71	2.33	2.43

The curve obtained by differential scanning calorimetry, for a heating rate of 5°C/min for amorphous $Fe_{71}Co_4Cr_1B_7Si_{17}$ alloy (Fig. 6) shows two peaks at about 428°C and 535°C which are the indication of some exothermic transformation [14]. For faster annealing conditions (heating rate at 10°C/min) only one peak was detected on the DSC curves, suggesting that the lower heating rate offers a more precise possibility to determine transformation temperatures [20, 21]. It was shown that the peak temperature increases as the heating rate increases, suggesting a dependence on the heating rate of the sample [22]. Thus a measure of thermal stability of an amorphous alloy is given by the crystallization temperature, T_x.

Heat treated samples of all amorphous $Fe_{75-x}Co_xCr_1B_7Si_{17}$ alloys (x=1, 4, 7, and 10 at.%) have been analyzed to point out the influence of the heat treatments on the electrical, magnetic and structural properties of above mentioned alloys. It is well known that Fe-Co based metallic glasses exhibit excellent electrical and magnetic properties. Fig. 7 shows the variation of the electrical resistivity versus temperature for the as quenched amorphous $Fe_{71}Co_xCr_1B_7Si_{17}$ alloy.

The electrical resistivity of the amorphous $Fe_{75-x}Co_xCr_1B_7Si_{17}$ alloys, (where x=1, 4, 7, and 10 at.%) is much higher than that of crystalline materials and it is in the same range as for the familiar nichrome alloys widely used as resistance elements in electric circuits. Another interesting characteristic of the electrical resistivity of the amorphous alloys used in this experiment is that it does not vary very much with temperature. The electrical resistivity of these alloys has slightly increased with increasing cobalt percentage, Table 2.

A change in slope of electrical resistivity is observed in Fig. 7 around 250°C. The electrical resistivity changes are probably determined by structural relaxation of the as – cast amorphous phase, which involves the annihilation of free volumes and the development of the short – range ordering of the amorphous structure [12].

However, a considerable drop of electrical resistivity is obvious at temperatures above 400°C, Fig. 7. This drop is due to the process of crystallization. In fact, this resistivity drop emphasizes a critical point of each measured alloy. The first obvious drop of electrical resistivity, which appears at temperature up to 425°C,

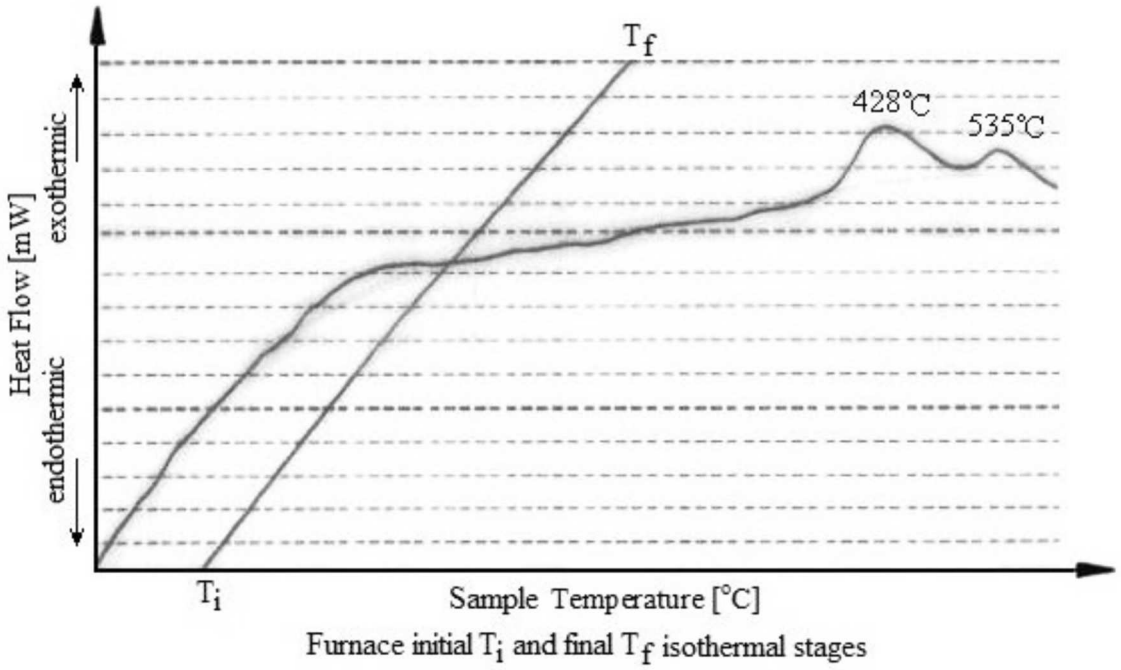

Fig. 6. DSC (differential scanning calorimetry) curve for the $Fe_{71}Co_4Cr_1B_7Si_{17}$ amorphous alloy

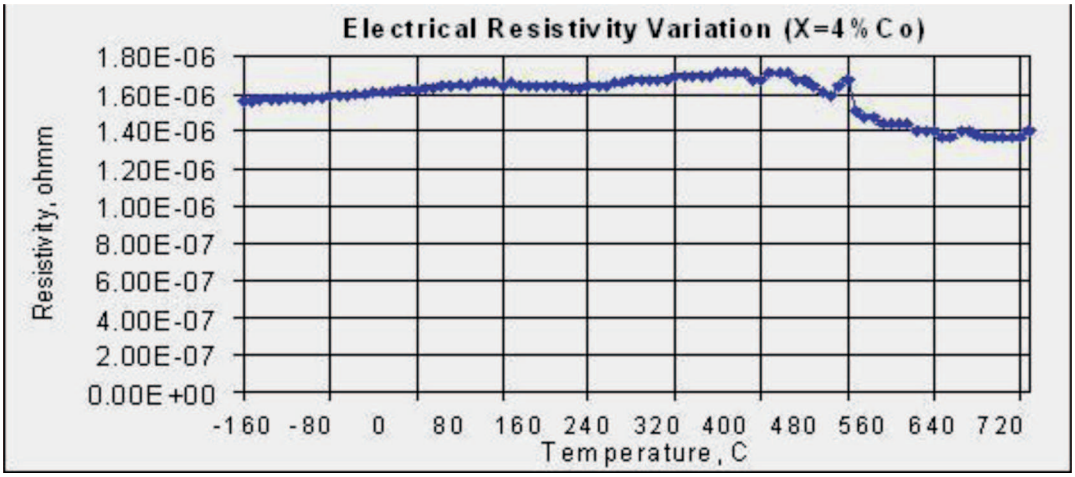

Fig. 7. Electrical resistivity variation of amorphous $Fe_{71}Co_4Cr_1B_7Si_{17}$ alloy as quenched versus temperature

corresponds to first crystallization stage on the DSC curve. The second drop corresponds to the second crystallization threshold at temperature of 525°C on the DSC curve. The experimental results suggest that the anomaly of the electrical resistivity is due to the amorphous state, more exactly due to crystallization of the residual amorphous matrix, which lead to formation of boride phases. Tacking into account the derivative curve of electrical resistivity versus temperature one can conclude that it matches very well with the DSC curve.

Due to their insensitivity to temperature variations for temperatures up to 400°C, these metallic glasses are suitable for applications in electronic circuits for which resistivity is an essential requirement [14, 23].

The electrical resistivity variation with annealing exposure time was also analyzed. In the case of the amorphous $Fe_{68}Co_7Cr_1B_7Si_{17}$ alloy (C3) annealed at 500°C for different holding times, 30, 60 and 90 min, respectively, one can see in Fig.8 that the electrical resistivity decreases with the increase of the exposure time. This is because starting with 450°C the structure of annealed samples contains evidence of crystalline precursors. The relative amount of crystalline phase Fe-Si is increased with an increase in temperature. At 500°C more crystalline phases, are formed with different iron configurations along with previous phases and relative amount of amorphous phase is further reduced. The crystalline

phases are FeSi and FeB with different numbers of iron atoms.

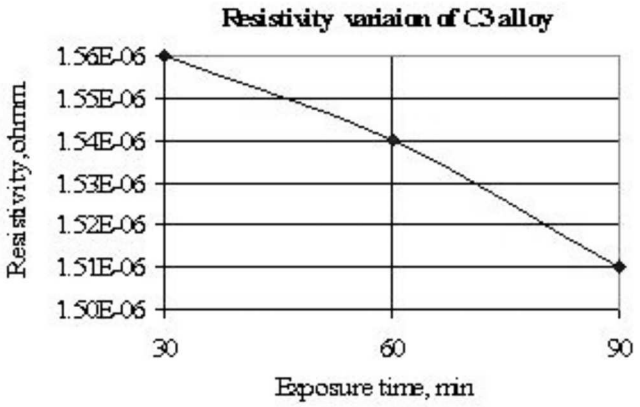

Fig. 8. Electrical resistivity versus annealing exposure time of the $Fe_{68}Co_7Cr_1B_7Si_{17}$ amorphous alloy (C3)

The annealed samples were also investigated by Vickers microhardness test. The microhardness variation with the heating temperature of the heat-treated samples is given in Table 3.

TABLE 3

Vickers microhardness variation with temperature

Temperature of heat treatment, °C	200	250	300	350	400	450	500
Vickers microhardness, HV	1086	973	965	890	865	920	958

The properties of $Fe_{68}Co_7Cr_1B_7Si_{17}$ alloy (C3) were significantly affected by structural relaxation, which is induced by annealing treatments conducted below transition temperature (Tg), at 200°, 250°, 300°, 350°, and 400°C. The structural relaxation induces a decrease of the loss factor since it produces a decrease of the defect concentration and then an increase of the local order. This reversible change could be due to short range chemical or topological ordering. The microhardness value corresponding to the relaxed state exhibits a slight decrease [24, 25], probably due to the change of local atomic and chemical configurations and due to the disappearance of FeSi nanocrystals in the temperature range [24]. The results indicate that the hardness increases at 450° and 500°C (partially crystallized samples) possibly due to the decrease of the free-volume and due to nucleation of Fe_3Si and α-Fe (Si) phases in amorphous matrix [19, 26, 27].

The influence of the holding time on the microhardness variation was also studied [15, 16]. Therefore, exposure times of 30, 60 and 90 minutes were applied in the case of the heat treatments at 300°C and 450°C. The microhardness variation with the exposure time of the applied heat treatments is shown in Table 4.

TABLE 4

Microhardness variation with holding time

Temperature of heat treatment, °C	Exposure time, min		
	30	60	90
300	968	907	901
450	995	1060	945

The microstructural and Roentgen analyses reveal that applying annealing at lower temperatures (i.e 300°C), even at longer times of exposure (60 or 90 minutes), does not modify significantly the initial structure. In Table 4 one can see that, irrespective of holding time, the microhardness increases with the increase of annealing temperature. This increase of microhardness of samples heat treated at 450°C can be attributed to the hard precipitates embedded in the amorphous matrix. However, the hardness at 450°C for 90 minutes holding time is smaller than the hardness at 300°C for 60 minutes holding time, probably due to appearance of more crystalline phases and decrease amount of amorphous phase [19, 25].

Fig. 9 shows microhardness variation with Co contain of the amorphous $Fe_{75-x}Co_xCr_1B_7Si_{17}$ alloys in as-cast state. One can see that for low Co percentage the microhardness first increased suddenly and then for Co percentage over 4 at.% it continued to increase very slightly.

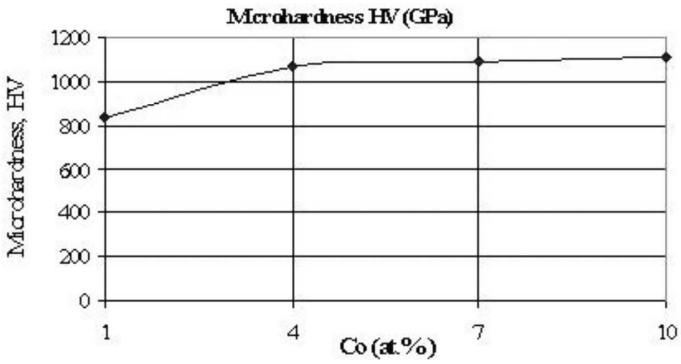

Fig. 9. Microhardness versus Co content of the $Fe_{75-x}Co_xCr_1B_7Si_{17}$ amorphous alloys

The changes in X-ray diffraction patterns and electric resistivity are a manifestation of the structural relaxation of the amorphous matrix when the amorphous $Fe_{75-x}Co_xCr_1B_7Si_{17}$ alloys were isothermal annealed below the glass transformation temperature (T<Tg). During isothermal annealing (T) below Tg (glass transition temperature), the glass tried to reach the ideal glassy state characteristic of the annealing temperature.

4. Conclusions

The amorphous nature of the samples was confirmed metallographic and by X-ray diffraction studies using Cu- Kα radiation. X-rays diffraction analysis showed that the alloy is in an amorphous state.

The electrical resistivity of amorphous $Fe_{75-x}Co_xCr_1B_7Si_{17}$ alloys (x=1, 4, 7, and 10 at.%), has slightly increased with increasing cobalt percentage.

Heat treated samples of all above mentioned amorphous alloys have been analyzed to point out the influence of heat treatments upon their electrical and structural properties.

A considerable drop of electrical resistivity is obvious at temperatures above 400°C. This drop is due to the process of crystallization. In fact, this resistivity drop emphasizes a critical point of each measured alloy. These critical points that could be also detected on the differential thermal analysis curves mutually coincide.

The diffraction analysis diagrams of the samples which were annealed below 450°C are identical and reveal only a structure typically to the amorphous state. In the case of the sample annealed at 450°C the structure is still predominantly amorphous, but shows evidence of crystalline precursors.

The microstructural and Roentgen analyses reveal crystals of some compounds after annealing at 500°C for 30 minutes. Applying annealing at lower temperatures, even at longer times of exposure (60 or 90 minutes) does not modify the structure. The number and size of FeB crystals increases with annealing time.

REFERENCES

[1] T. Komatsu et al., Acta Metall. **34**, 1899-1904 (1986).
[2] R. Nowosielski et al., J. Achievements in Mater. and Manuf. Eng. **30**, 135-140 (2008).
[3] M.F. Ashby, A.L. Greer b, Scripta Materialia **54**, 321-326 (2006).
[4] L.F. Barquin et al., Phys. Stat. Sol. **155**, 439 (1996).
[5] O. Touraghe et al., Phys. B **403**, 2093-2096 (2008).
[6] D.F. Jones et al., Mat. Sci. Eng. **99**, 207-210 (1988).
[7] K. Pekala et al., J. Non-Cryst. Solids **347**, 27-30 (2004).
[8] A. Hsiao et al., IEEE Transactions on Magnetics **38**, 3039 (2002).
[9] D.A Rein, R.A Levi, vol. Magnetism amorfnah sistem, Moskva, Mettalurghia 1981.
[10] J. Perez, F. Fouquet, G. Lormand, Proprietes mecaniques des verres metalliques, Les amorphes metalliques, Aussois, Les Edition de Physique, France 1983.
[11] Y. Hu, Lin Liu, K.C. Chan, M. Pan, W. Wang, Mater. Lett. **60**, 1080-1084 (2006).
[12] H.H. Liebermann, Rapidly solidified alloys: processes, structures, properties, applications, Marcel Dekker, New York 1993.
[13] R. Zallen, The Physics of Amorphous Solids, John Wiley & Sons, 1998.
[14] I. Solomon, PhD Thesis, University of Galati, Romania 1998.
[15] K.V.P.M. Shafi, A. Gedanken, J. Appl. Phys. **81**, 6901- 6905 (1997).
[16] G. Zhang, W. Liu, H. Zhang, Chinese Phys. Lett. **8**, 86 (1991).
[17] Yi Liu, D.J. Sellmyer, D. Shindo, Handbook of advanced magnetic materials, Tsinghua University Press, Springer 2001.
[18] D. Querlioz, E. Helgren, D.R. Queen, F. Hellman, Appl. Phys. Lett. **87**, 221901 (2005).
[19] A. Quivy et al., Acta Metall. **32**, 1527 (1984).
[20] H.F. Li, D.E. Laughlinz, R.V. Ramanujan, Philos. Mag. **86**, 1355-1372 (2006).
[21] D.R. dos Santos, D.S. dos Santos, Mater. Research **4**, 47-51 (2001).
[22] Hai Ni, H.-J. Lee, A.G. Ramirez, J. Mater. Res. **20**, 1727-1734 (2005).
[23] C.K. Kim et al., Mater. Sci. and Eng. **B76**, 211-216 (2000).
[24] X. Li et al., J. Mater. Sci. Technol. **23**, 253-256 (2007).
[25] J.I. Akhter et al., J. Mater. Sci. Technol. **25**, 48-52 (2009).
[26] G. Zha, A. Zhang, J. Rare Earths **28**, 243-245 (2010).
[27] M.L. Vaillant et al., Scripta Materialia **47**, 19-23 (2002).

Received: 10 February 2012.